CHAPTER 95

Wave-Current Interaction in Inlets

Michael J. Briggs[1], Zeki Demirbilek[1], and Debra R. Green[2]

ABSTRACT

Laboratory experiments were conducted in a flume to study wave-current interaction at the entrance to an inlet. Regular and irregular waves were studied with and without ebb and flood currents. These data are being used to develop a parameterization of the wave breaking criterion in the presence of currents in inlets, provide guidance to the field on the effects of currents on waves, and improve the predictive capability of numerical models for enhancing navigation in inlets.

INTRODUCTION

The coastal zone involves interactions between winds, waves, currents, structures and sediment. To develop a sound coastal management plan for shoreline stabilization and protection near inlets and improve navigation safety, it is essential to have a better understanding of the complicated physics which occur between waves and currents in coastal waters. In the vicinity of tidal inlets and river mouths, currents can significantly modify wave amplitudes, form, and directions. Although wave-current interaction has been studied extensively, little design guidance exists for its effect on wave breaking.

In 1993 the U.S. Army Engineer Waterways Experiment Station's Coastal Engineering Research Center began a large research program entitled the Coastal Inlets Research Program (CIRP). One of the goals of this program is to better understand wave-current interaction in the vicinity of coastal inlets and to develop a wave model that will be an integral part of an Inlet Modeling System (IMS) for numerically modeling waves, currents, and sediment transport over relatively short temporal and spatial scales. Part of this effort involves conducting laboratory studies of wave-current interaetion to develop an empirical wave

[1]Research Hydraulic Engineer, Coastal and Hydraulics Laboratory, USAE Waterways Experiment Station, 3909 Halls Ferry Rd., Vicksburg, MS 39180-6199.

[2]Computer Specialist, Coastal and Hydraulics Laboratory, USAE Waterways Experiment Station, 3909 Halls Ferry Rd., Vicksburg, MS 39180-6199.

breaking criterion for waves in the presence of ebb and flood currents.

This paper presents an overview of a CIRP flume experiments and results from an initial analysis of some of the ebb current data. The first section gives a brief summary of some previous flume and basin experiments involving wave-current interaetion. The next section gives a comprehensive description of the flume experiments including model setup, wavemaker, current system, instrumentation, and cxperimental program. The final section presents and discusses some of thc preliminary analyses of the flume data for eight representative, wave-ebb current cases.

BACKGROUND

Sakai and Saeki (1984) measured the effect of opposing currents on wave height transformation over a 1:30 sloping beach for a range of wave periods and steepness. They found an increase in wave height and decay rate in the presence of the opposing current. Lai et al. (1989) conducted flume experiments on the kinematics of wave-current interactions for strong interactions with waves propagating with and against a current. They found the influenee of the waves on the mean current profiles was small, although opposing waves would give a slightly lower current. They also observed a drastic change in the spectral shape, especially the higher harmonics, following wave breaking in the presence of opposing currents. Their experiments confirmed that blockage of waves by a current (when the wave group velocity equals the opposing current velocity) occurs when the ratio of depth-averaged current velocity to wave celerity without currents approaches 0.25.

Yucheng et al. (1991) and Yucheng and Guohai (1993) noted that breaker indices for finite water depth for regular and irregular waves in the presence of opposing currents can be classified by geometric, kinematic, and dynamic criteria. Typical geometric stability criteria include McCowan's critical crest angle $\beta=120$ deg, Longuet-Higgin's limiting wave surface slope of about 30.4 deg, McCowan's wave breaking index $\kappa=0.78$, Miche's limiting wave steepness value $H_b/L_b=0.142 \tanh kh$, and Goda's limiting relative wave height H_b/h_b as a function of relative water depth h/L_0 and bottom slope m. The kinematic stability parameter is based on the concept that the horizontal water particle velocity u is equal to the wave celerity C at breaking. The dynamic stability criterion relates the vertical acceleration of the water particles in the crest at breaking to a limiting value. They found that the two geometric criteria of limiting wave steepness H_b/L_b and limiting relative wave height H_b/h_b are consistent and stable with values of $H_b/L_b=0.129$ for irregular spilling breakers with and without currents on a gentle slope.

Briggs and Liu (1993) conducted laboratory experiments of the interaction of ebb currents with regular waves on a 1:30 beach and entrance channel. Good agreement was obtained between these data and numerical model predietions. They found little effect on wave period, but significant increases in wave height and nonlinearity. Raichlen (1993) conducted a laboratory investigation on the propagation of regular waves on an adverse three-dimensional jet. He found increases in incident wave height by a factor of two or more for ebb current to wave celerity (i.e., U/C) values as small as 10 percent.

Suh et al. (1994) developed an equation for the equilibrium-range spectrum of waves propagating on an opposing current in finite depth water. Comparison with experimental data agreed reasonably well with the change in high-frequency energy in the wave spectrum.

Klopman (1994) conducted a series of flume experiments to study flow kinematics of regular and irregular waves in the presence of ebb and flood currents. He found that waves opposing the current increase the horizontal velocity in the upper half of the water column and that this change depends mainly on wave energy and less on the shape of the wave spectrum.

EXPERIMENTAL DESIGN

Model Setup

A 1.5-m-wide, 1.5-m-deep, 64-m-long flume (Figure 1) was used to simulate a three-dimensional flow environment by partitioning the down-wave end of the flume with a temporary vertical wall into an 18-cm-wide, 7.2-m-long channel. Turbulence (due to the ebb currents transitioning from the full width of the flume into the narrower channel) was minimized by a 2.8-m-long, convex-shaped transition zone on the landward side of the channel. Water depth in the flat-bottomed flume was 50 cm. A 14.6-m-long glass window allowed observation in the study area.

The x-axis extended longitudinally down the centerline of the channel from the seaward end of the partition wall or channel entrance at $x=0$. The y-axis origin was at the channel centerline and extended laterally towards the wide part of the flume.

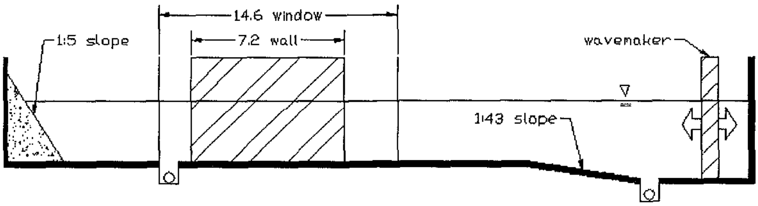

Figure 1. Layout of wave-current flume.

Wavemaker

The hydraulic wavemaker was located 39.6 m from the origin at the channel entrance. It has an 86 cm maximum stroke and is driven in translational motion (i.e., piston mode) by a Digital MicroVax minicomputer. It is submerged 46 cm lower than the floor of the flume, separated by a 20.4-m-long, 1:43 slope. Wave absorption was provided by a 1:5 rock beach on the back wall of the flume and a 1:6 rock beach and several rolls of horsehair on the seaward side of the channel partition.

Current System

Ebb and flood currents were generated with a circulation system consisting of two inflow/outflow boxes, a pump, a pipe manifold, flow meter, and return pipe. The inflow/outflow boxes were separated a distance of 48.1 m and located below floor level at each end of the flume. Each box had a total volume of 0.89 m^3, measuring 1.07 m long, 1.37 m wide, and 0.61 m deep. A 20-cm-diameter manifold pipe was suspended across the width of the flume in each box to distribute the flow evenly while minimizing wave disturbance and flow turbulence. Radial cuts extending ± 70 deg from the bottom of the pipe, rather than perforations, were used to increase the cross-sectional area of the manifold to reduce vertical flow velocities to less than 3 cm/s.

The pump and pipe manifold were located midway between the inflow/outflow boxes to minimize flow resistance. A Goulds horizontal split-case centrifugal pump, with a maximum discharge of 126 l/s, was at the center of the manifold. The manifold consisted of 25.4-cm-diameter PVC pipe and ball valves to reverse the flow from ebb to flood. Flow discharge was controlled by an electrically actuated butterfly valve and measured by a Dynasonics clamp-on ultrasonic transit time flowmeter. Typical accuracy of this meter is 1 percent. The return pipe on either side of the manifold was also 25.4-cm-diameter PVC pipe.

Table 1
Wave Gage Locations

Gage	*x*, m	*y*, m	*x/w*	*y/w*
W1	0.91	0	5	0
W2	1.83	0	10	0
W3	2.74	0	15	0
W4	3.66	0	20	0
W5	4.57	0	25	0
W6	5.49	0	30	0
W7	6.40	0	35	0
W8	7.32	0	40	0
W9	8.23	0	45	0
W10	9.14	0	50	0
W11	10.06	0	55	0
W12	1.83	0.37	10	2
W13	2.74	0.37	15	2
W14	3.66	0.37	20	2
W15	4.57	0.37	25	2
W16	5.49	0.37	30	2
W17	9.14	0.37	50	2
W18	2.74	0.73	15	4
W19	4.57	0.73	25	4
W20	5.49	0.73	30	4

Instrumentation

Wave gages. Surface elevations were measured by twenty capacitance wave gages in a 10-m by 0.7-m measurement area, bounded by the channel centerline and the origin at the channel entrance. Eleven of the twenty gages were located along the channel centerline in Row 1. The remaining gages were located on two parallel cross-shore transects: six in Row 2 and three in Row 3. Gage spacing was 91 cm in the x-direction and 37 cm in the y-direction. These spacings corresponded to normalized channel widths of 5 *x/w* and 2 *y/w*, respectively, where *w* is the channel width. Table 1 lists gage locations and normalized distances.

Current meters. Seven acoustic Doppler current meters were used to calibrate ebb and flood currents and quantify the wave-current interaction effect. These current meters are manufactured by Sontek. The system consists of a measurement probe and stem, signal conditioning and processing modules, and a 486 PC.

Incident ebb current flows were measured by two meters positioned inside the channel along the centerline. The meter at the channel entrance was the primary meter, with the interior meter serving in a backup role. Because it was not physically possible to co-locate current meters and wave gages, they were positioned between wave gages along all three transects: two on each of the first two transects and one on the third transect. Table 2 lists meter positions and normalized *x/w* and *y/w* distances.

Table 2
Current Meter Locations

Meter	*x*, m	*y*, m	*x/w*	*y/w*
C1	-1.83	0.00	-10.0	0
C2	0.00	0.00	0.0	0
C3	2.29	0.00	12.5	0
C4	3.20	0.00	17.5	0
C5	2.29	0.37	12.5	2
C6	3.20	0.37	17.5	2
C7	3.66	0.73	20.0	4

Measurements were made at a depth equal to 0.4 times the depth from the bottom of the flume. This depth corresponds approximately (0.37 factor) to a logarithmic profile for the depth-averaged velocity. This depth was a compromise to ensure that the current meter remained submerged for all wave troughs while providing clearance for the largest wave crests.

Positive u- and v-velocities were oriented in the positive x- and y-axis directions, respectively. Five of the meters measured u-, v-, and w-velocities. However, only those in the horizontal plane were analyzed for this study.

Experimental Program

Wave and current conditions. A total of over 160 cases, representative of wave and current conditions in a typical inlet, were studied. Cases consisted of 12 irregular waves, 6 regular waves, 3 ebb current, 3 flood current, and 96 wave-current combinations. Only the irregular wave and ebb current results are presented in this paper. Table 3 lists corresponding model and prototype values for water depth, and wave and current parameters, based on a model-to-prototype scale of 1 to 20.

Table 3
Wave and Current Parameters

Quantity	Model	Prototype
Water depth	50 cm	10 m
Wave Period	1.57 s	7 s
	2.24 s	10 s
	3.35 s	15 s
Wave Height	5 cm	1 m
	10 cm	2 m
	15 cm	3 m
Ebb Current	11.2 cm/s	0.5 m/s
	22.4 cm/s	1.0 m/s
	44.7 cm/s	2.0 m/s

Wave calibration. The target frequency spectrum for the model waves was based on the Texel Marsden Arsloe (TMA) spectrum (Bouws et al. 1985). The TMA spectrum is a function of five parameters: peak frequency, Phillip's constant, peak enhancement factor, lower and upper spectral width parameters σ_l and σ_u , and water depth h. Although identical to the JONSWAP spectrum in deep water, the TMA is modified by a depth-correction factor in shallow water. Peak enhancement factors of 2 and 10 were chosen to simulate sea and swell frequency spreading, respectively. Values of $\sigma_l=0.07$ and $\sigma_u=0.09$ were used for all irregular waves. The Phillip's

Table 4
Calibrated Wave Heights

Case	Target, cm	Gages 1-11, cm	% Dev	Gages 1-20, cm	% Dev
1	5	5.00	0.00	4.97	0.60
2	10	10.12	1.20	10.04	0.40
3	15	14.94	0.40	14.82	1.20
4	5	4.96	0.80	4.94	1.20
5	10	9.88	1.20	9.82	1.80
6	15	15.08	0.53	14.98	0.13
7	5	5.00	0.00	4.98	0.40
8	10	9.99	0.10	9.96	0.40
9	15	14.93	0.47	14.88	0.80
A	5	5.02	0.40	4.97	0.60
B	10	10.04	0.40	9.96	0.40
C	15	14.94	0.40	14.86	0.93

constant was calculated based on the target zero-moment wave height H_{m0}.

Control signal durations of 2,000 s were created for each wave case. Data were collected for 1,000 s at a sampling rate of 10 Hz after a waiting time of 60 s to allow the slowest traveling wave to reach the farthest wave gage (W1).

Single channel frequency spectral analysis was used for the data analysis. Data records of 1,000 s were zero-meaned, tapered by a 10% cosine bell window, Fourier transformed, and band averaged, yielding a frequency resolution of 0.05 Hz with 100 degrees of freedom. Values for H_{m0} were computed for all cases.

Two or three iterations were required for each wave case to obtain target values. In general, the agreement between measured and target wave period, wave height, and spectral shape was very good. Table 4 compares measured and target H_{m0} for the 12 irregular wave cases for the average of the 11 gages on the centerline and all 20 gages. The percent deviation between measured and target values is also listed. Overall agreement is excellent for all cases, with a maximum variation of 1.2 percent for the centerline gages and 1.8 percent for all gages.

Current calibration. Software on the PC allowed real- time observation of the current time series and magnitudes. Current data were also collected for 1,000 s, but at a sampling rate of 25 Hz.

Prior to sampling, water was circulated for approximately 30 min to allow the current to reach a steady-state condition. This time is equivalent to 3-5 cycles of the slowest current traveling between inflow/outflow boxes. Seeding was added to the water and mixed to improve the signal-to-noise ratio of the current meters to acceptable levels. Initial calibration of each current condition required an iterative procedure of adjusting the flow control valve and waiting to re-establish steady-state conditions before continuing. After successfully matching the target velocity, the settings of the valve were recorded for future runs.

A current-only case was run first each day. Then, the 12 wave-current combinations for that current were run sequentially with approximately 5 min between each run for the flume to reach steady-state conditions prior to the next run. At the end of each day, the current-only run was repeated as a check on the current stability. The current repeatability was very good during a day's runs.

RESULTS AND ANALYSES

In this section, discussions of the current distribution, current-modified wave parameters, wave amplification, and spectral evolution are presented for eight representative cases. These cases consist of two wave periods (T=1.57 and 2.24 s), two wave heights (H=5 and 15 cm), and two ebb currents (U=11.2 and 44.7 cm/s). They correspond to prototype wave and current conditions of T=7 and 10 s, H=1 and 3 m, and U=0.5 and 2.0 m/s, respectively. Only wave gage and current meter data from the channel centerline are considered in this paper.

Current Distribution

As the ebb current exits the channel it decreases in magnitude and spreads out laterally within the confines of the flume side walls. Figure 2 shows the measured ebb current along the channel centerline for each of the eight wave-current cases. The value for U is plotted versus normalized distance x/w (i.e., equivalent number of channel widths w) seaward of the channel entrance for the T=1.57 s cases in the top panel and T=2.24 s cases in the bottom panel. All current values are interpolated or extrapolated from the three current measurement locations on the channel centerline.

The stronger ebb currents are felt by the waves at a larger x/w distance from the channel entrance. At this distance, the wave celerity effectively overpowers the current and it

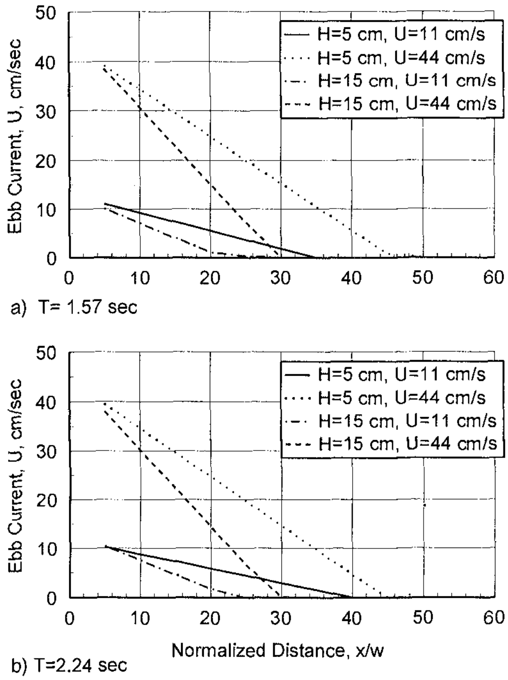

Figure 2. Current distribution.

vanishes. Waves with larger wave heights reduce the current closer to the mouth of the channel, effectively changing the current field.

Wave Parameters

Wave parameters are modified by the presence of a steady, uniform ebb current U. The apparent or absolute wave frequency σ_a and celerity C_a of the wave traveling on the current are reduced relative to their intrinsic or calm water values (i.e. σ_i and C_i) when an ebb current is not present. The wavelength L and wavenumber k remain fixed, however. These relationships are given by

$$\sigma_a = \sigma_i + kU\cos\theta \quad (1)$$

$$C_a = C_i - U \quad (2)$$

where θ =the angle between the direction of wave propagation and that of the ebb current, which is 180 deg in our case. Thus, the absolute wave period T_a $(=2\pi/\sigma_a)$ for waves on an ebb or opposing current is increased or stretched relative to the intrinsic period T_i $(=2\pi/\sigma_i)$. Also, the wave height H and wave steepness H/L are increased. Table 5 lists intrinsic values for the eight cases, based on linear wave theory. The first digit in the "Case" ID corresponds to the wave case from Table 4 and the second digit to the current magnitude.

The numerical wave model REFDIF, a combined refraction-diffraction, parabolic approximation model, was used for computing changes in wave parameters due to ebb and flood currents (Kirby and Dalrymple 1994). Using the flume geometry and measured current data, current-modified wave parameters were calculated with this model. Irregular waves

Table 5
Intrinsic Wave Parameters

Case ID	T_i, s	H, cm	U, cm/s	C_i, cm/s	U/C_i	H/L
11	1.57	5	11.2	191	0.06	0.005
13			44.7		0.23	0.005
31	1.57	15	11.2		0.06	0.050
33			44.7		0.23	0.050
41	2.24	5	11.2	207	0.05	0.011
43			44.7		0.22	0.011
61	2.24	15	11.2		0.05	0.032
63			44.7		0.22	0.032

were modeled as equivalent regular waves corresponding to the peak period with $H_{rms}=H_{m0}/\sqrt{2}$.

The change in H/L as a function of U/C_a for each of the eight cases is shown in Figure 3. Values for H/L are calculated by dividing the measured wave height by the predicted wavelength from the REFDIF wave model. The U/C_a values correspond to the different gage locations along the channel centerline. Wave steepness increases by a factor of two for all the cases, and as much as an order of magnitude for case 11 (i.e., T=1.57 s, H=5 cm, U=11.2 cm/s).

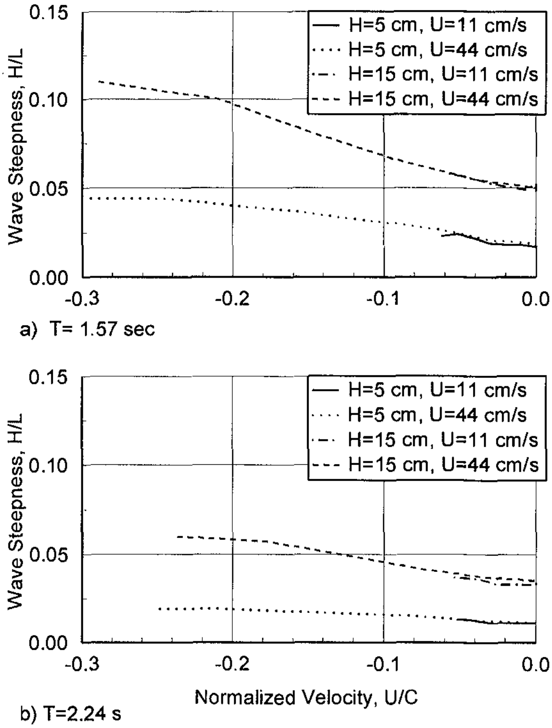

Figure 3. Current effect on wave steepness

Wave Amplification

Figure 4 shows wave amplification H/H_i versus normalized distance x/w for the eight cases. Measured wave height H was divided by incident wave height H_i for the wave-only condition at each location for each case to obtain values of H/H_i.

The largest amplification occurred for the T=1.57 s cases (top panel), and for the largest ebb current for both wave periods. Wave height increased by almost a factor of two for case 13 with the larger current. Maximum amplification was somewhat smaller for the T=2.24s cases shown in the bottom panel, on the order of 1.5.

Spectral Transformation

As waves propagate toward the channel entrance, they are affected by the ebb current more strongly. This is manifested in the growth of the higher frequency components. The wave may initially experience gentle or occasional breaking due to blockage of these higher frequency waves, with correspondingly increased wave steepness. The higher frequency components are reduced relative to those previously present. The total energy in the spectrum, however, does not decrease appreciably. According to Lai et al. (1989), the peak frequency may be Doppler shifted to a lower value. Suh et al. (1994), however, did not observe this phenomenon in their experiments.

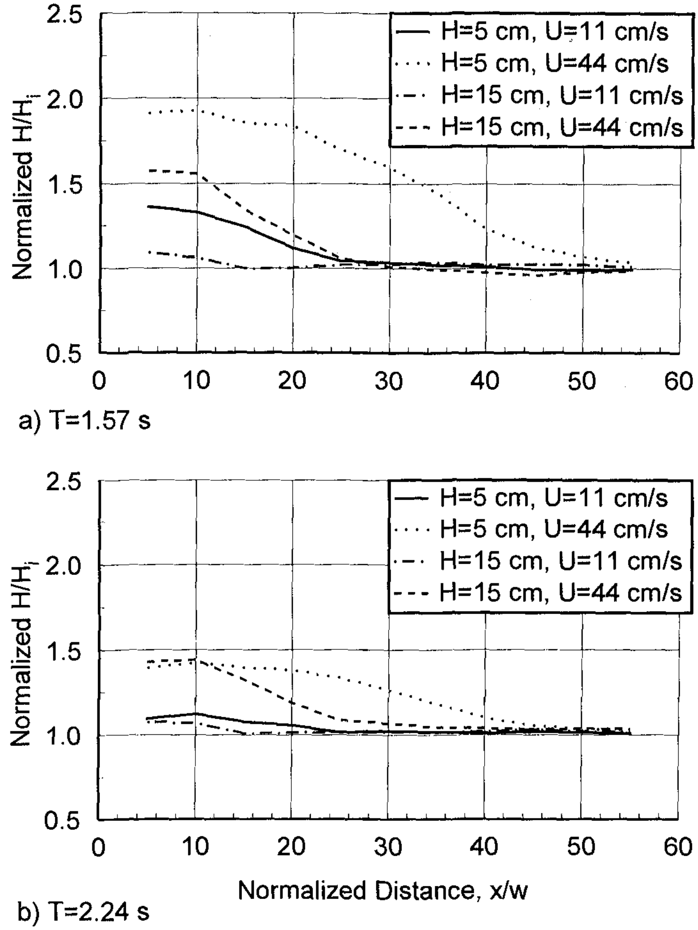

Figure 4. Wave amplification effect.

In a severe breaking environment, however, the spectral shape may change appreciably. The higher frequency components of the spectrum are often completely blocked, resulting in violent breaking and drastic change in the spectral shape. The high-frequency half of the spectrum above the spectral peak may be reduced an order of magnitude relative to its wave-only condition. The peak frequency may be reduced as well.

Figures 5 and 6 are semi-log plots of the measured frequency spectra for wave-only and wave-current conditions for wave periods of T=1.57 and T=2.24s, respectively. Gage positions 1 through 6 are shown for x/w equivalent to (a) 5, (b) 10, (c) 15, (d) 20, (e) 25, and (f) 30. The incident wave height is H=15 cm in all plots. In each plot, the dotted line corresponds to the wave-only condition at x/w=55 (i.e., gage 11), the solid line to the wave-current condition with U=11.2 cm/s current, and the dot-dash line to the U=44.7 cm/s case.

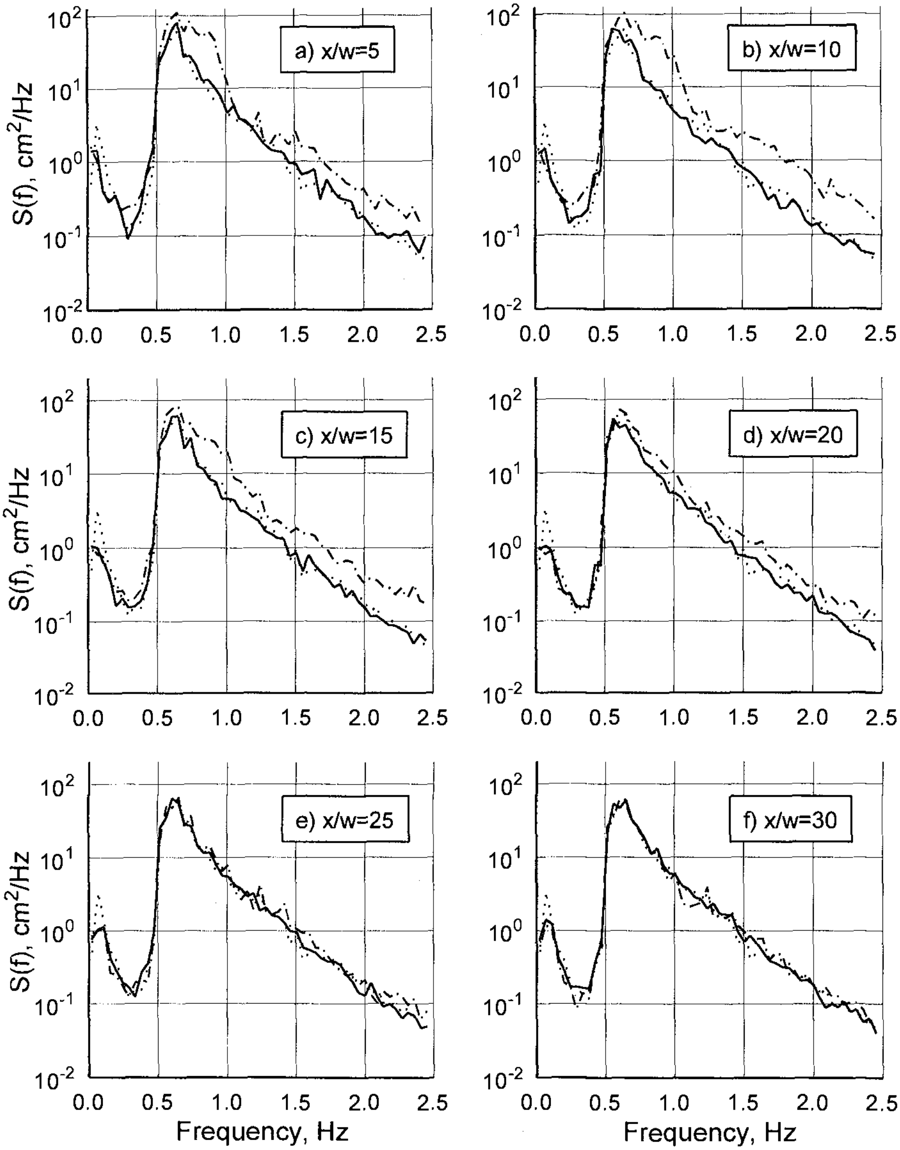

Figure 5. Spectral evolution for $T=1.57$ s, $H=15$ cm cases for $x/w=5$ to 30. Dotted line is wave-only, solid line is $U=11$ cm/s, and dot-dash line is $U=44$ cm/s.

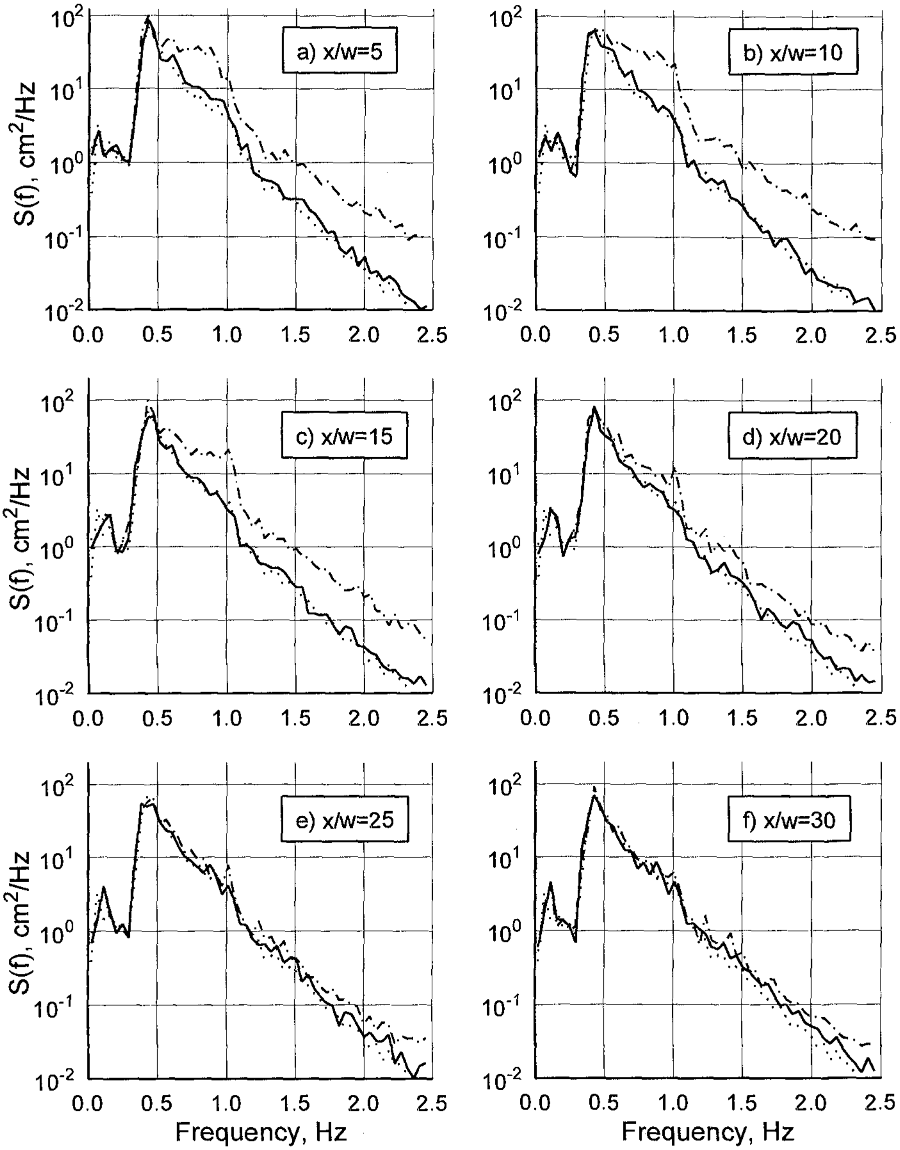

Figure 6. Spectral evolution for T=2.24 s, H=15 cm cases for x/w=5 to 30. Dotted line is wave-only, solid line is U=11 cm/s, and dot-dash line is U=44 cm/s.

For the T=1.57 s cases, the U=11.2 cm/s ebb current has little effect on the spectral shape. The wave celerity is much stronger than the current velocity, on the order of U/C_a=-0.06 (see Table 5 and Figure 3). The larger current (U/C_a=-0.23), however, does have an effect on this wave. Initially, there is little effect, but at x/w=20 the higher frequency components increase, reaching a maximum at x/w=10. Gentle breaking then occurs between x/w=5 and 10, as evidenced by the decrease in the higher frequency components. This is in agreement with the H/L and U/C_a values predicted by the numerical model and the observations of Lai et al. (1989) that the wave blockage limit is approximately $U/C_a \leq$ -0.25. There does not appear to be any obvious frequency shifting in the peak frequency, however.

For the T=2.24 s cases, again there is no significant effect of the current on the wave spectrum. The U/C_a ratio is on the same order as before. The larger current U=44.7 cm/s case causes a growth of higher frequency components, much like the previous case. The decrease in this frequency range is less than before with the most significant decrease occurring between 1.25 and 1.50 Hz. Occasional breaking was observed in this case between x/w=5 and x/w=15.

These increases in the higher-frequency components of the wave spectra are much like what was observed by Briggs and Smith (1990) and Smith and Vincent (1992) due to shoaling alone. The ebb current appears to enhance this nonlinear growth of the higher harmonics.

CONCLUSIONS

Laboratory experiments were conducted in a flume to study wave-current interaction at the entrance to an inlet. Regular and irregular waves were studied with and without ebb and flood currents. This paper presents an overview of the experiments and results from an initial analysis of some of the ebb current data. Gentle or occasional wave breaking was observed in the larger wave height cases. A numerical wave model was used to predict the effect of the current on the wave parameters. The agreement with these predictions and model measurements with previous experiments was very good. Ebb currents tend to enhance the nonlinear growth of higher-harmonic components, much like shoaling on a beach. Additional research with this data is in progress to develop a current-induced wave breaking criterion, provide guidance to the field on the effects of currents on waves, and improve the predictive capability of numerical models for enhancing navigation in inlets.

ACKNOWLEDGMENTS

The authors wish to acknowledge Headquarters, U.S. Army Corps of Engineers, for authorizing publication of this paper. It was prepared as part of the "Modeling Waves at Inlets" work unit in the Coastal Inlets Research Program. We would like to thank Messrs. Dave Dailey, Jeremy Mucha, and John Evans for their help during this project.

REFERENCES

Bouws, E, Gunther, H, Rosenthal, W, and Vincent, C (1985). "Similarity of the Wind Wave Spectrum in Finite Depth Water," *J Geophys Res*, Vol 90, No C1, pp 975-986.

Briggs, MJ, and Smith, JM (1990). "The Effect of Wave Directionality on Nearshore Waves," *Proc 22nd ICCE Conference,* Delft, The Netherlands, 2-6 Jul, pp 267-280.

Briggs, MJ, and Liu, PLF (1993). "Experimental Study of Monochromatic Wave-Ebb Current Interaction," *Proc Waves '93 Conference,* New Orleans, LA, Jul, pp 474-488.

Kirby, JT, and Dalrymple, RA (1994). "Combined Refraction/Diffraction Model REFDIF 1," *CACR Report No. 94-22*, Cntr for Appl Coastal Res, Univ Delaware, pp 77.

Klopman, G (1994). "Vertical Structure of the Flow Due to Waves and Currents," *Progress Report H 840.30, Part II,* Delft Hydraulics, The Netherlands, Feb, pp 1-38.

Lai, RJ, Long, SR, and Huang, NE (1989). "Laboratory Studies of Wave-Current Interaction: Kinematics of the Strong Interaction," *J Geophysical Research*, Vol 94, No C11, November, pp 16,201-16,214.

Raichlen, F (1993). "Waves Propagating on an Adverse Jet," *Proc Waves '93 Conference,* New Orleans, LA, Jul, pp 657-670.

Sakai, S, and Saeki, H (1984). "Effects of Opposing Current on Wave Transformation on a Sloping Bed," *Proc 19th Conf. on Coastal Engineering*, ASCE, Vol 1, pp 1132-1148.

Smith, JM, and Vincent, CL (1992). "Shoaling and Decay of Two Wave Trains on Beach," *J Waterway, Port, Coastal, and Ocean Engineering,* ASCE, Vol 118, No 5, Sep/Oct, pp 517-533.

Suh, KD, Kim, YY, and Lee, DY (1994). "Equilibrium Range Spectrum of Waves Propagating on Currents," *J Waterway, Port, Coastal, and Ocean Engineering*, ASCE, Vol 120, No 5, Sep/Oct, pp 434-450.

Yucheng, L., Guohai, D., and Bin, T. (1991). "Wave Breaker Indices in Finite Water Depth," *China Ocean Engineering*, Vol 5, No 1, pp 51-64.

Yucheng, L. and Guohai, D. (1993). "Wave Breaking Phenomena of Irregular Waves Combined with Opposing Current," *China Ocean Engineering*, Vol 7, No 2, pp 197-206.